

CPT-based Multifunctional Grid-Tied Inverter with Type II Controller

Tiago Davi Curi Busarello (UFSC), José de Arimatéia O. Filho (UNESP/ICTS), Alex Ferreira Silva (UNESP/ICTS), Paulo Fernando Silva (UNESP/ICTS), Helmo Kelis Morales Paredes (UNESP/ICTS)

I. INTRODUCTION AND METHODOLOGY

The increasing penetration of Distributed Energy Resources (DERs), such as photovoltaic and wind energy systems, in microgrids and smart grids imposes significant challenges for maintaining power quality and system stability, including voltage distortions, unbalances, and improper power injection. In this context, the Multifunctional Grid-Tied Inverter (MFGTI) emerges as a critical device, capable of simultaneously managing active power injection and compensating power quality issues. To address these challenges, this paper proposes the implementation of a Type II controller in the current loop of the MFGTI, ensuring implementation simplicity and compliance with regulatory standards. The reference current is generated using the Conservative Power Theory (CPT) combined with a Phase-Locked Loop (PLL), enabling selective compensation of disturbances while concurrently injecting active power into the utility grid. Simulation results obtained using TyphoonSim® under various operating conditions confirm the effectiveness of the proposed approach, demonstrating precise reference tracking, reliable operation, and mitigation of distortions, thus supporting efficient DER integration and stable microgrid performance.

Fig. 1 shows a typical structure of a single-phase MFGTI with an LC filter connected to the grid, where the term V_{dc} is a bidirectional DC link accoupled to voltage at the Point of Common Coupling (PCC). The uncontrolled Open-loop Transfer Function, $OLTF_u$, can be expressed as (1). To design the controller, the phase and gain values at the desired cutoff frequency are obtained from the $OLTF_u$, as expressed in (2) and (3), respectively.

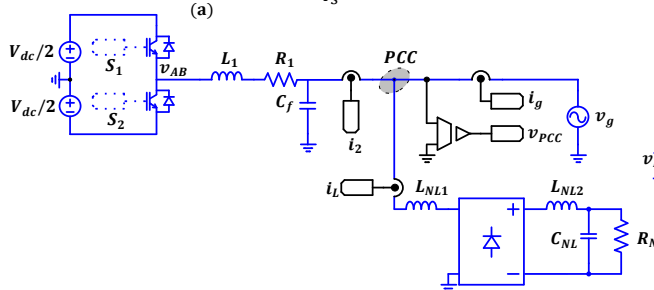
$$OLTF_u(s) = PWM(s) \cdot \frac{V_{dc}}{L_f s + R_f} \cdot K_i \quad (1)$$

$$\varphi_{sl} = \angle OLTF_u(f_c) [^\circ] \quad (2)$$

$$G_{Sl_{dB}} = |OLTF_u(f_c)| [dB] \quad (3)$$

The Type-II current controller, $G_i(s)$, is an integral single-lead digital current controller, having a pole at the origin and single zero-pole pairs [1]. Its transfer function in the z-domain, given by (4) and (5):

$$G_i(z) = G_i(s) \Big|_{s=\frac{1-z^{-1}}{T_s}} \quad (4)$$



$$G_i(z) = \frac{b_0 + b_1 z^{-1} + b_2 z^{-2} + b_3 z^{-3}}{a_0 + a_1 z^{-1} + a_2 z^{-2} + a_3 z^{-3}} \quad (5)$$

The coefficients of the digital current controller are determined by the following equations, along with the definition of five constants, denoted as D_1 through D_5 :

$$D_1 = R_2 C_1 C_3 (R_1 + R_3) \quad (6)$$

$$D_2 = R_2 C_1 + R_1 C_3 + R_3 C_3 \quad (7)$$

$$D_3 = R_1 R_2 R_3 C_1 C_2 C_3 \quad (8)$$

$$D_4 = R_1 R_2 C_1 (C_1 + C_2) + R_1 R_2 C_1 C_2 \quad (9)$$

$$D_5 = R_1 (C_1 + C_2) \quad (10)$$

$$\beta = D_3 + D_4 T_s + D_5 T_s^2 \quad (11)$$

$$b_0 = \frac{T_s D_1 + D_2 T_s^2 + T_s^3}{\beta} \quad (12)$$

$$b_1 = -\frac{2 T_s D_1 + D_2 T_s^2}{\beta}, b_2 = -\frac{T_s D_1}{\beta} \quad (13)$$

$$a_1 = -\frac{3 D_3 + 2 D_4 T_s + D_5 T_s^2}{\beta_{dl}} \quad (14)$$

$$a_2 = \frac{3 D_3 + D_4 T_s}{\beta}, a_3 = -\frac{D_3}{\beta} \quad (15)$$

The CPT consists of a mathematical formulation to characterize physical phenomena observed in single-phase and polyphase electrical circuits with non-sinusoidal source voltages [2]. It is also applied to the control MFGTI for power factor (λ) compensation, enabling the partial mitigation of disturbances. Thus, by measuring the current of a generic load i_L and the voltage at the PCC, between the MFGTI and the grid, CPT decomposes i_L as [2], [3]:

$$i_L = i_a + \underbrace{i_r}_{i_{na}} + i_v = i_a + i_{na} \quad (16)$$

where i_a is the active current, i_r is the reactive current, and i_v is the void (distortion) current, each one associated with a specific physical phenomenon, and i_{na} is the non-active current. The orthogonal decomposition of currents via CPT results in different components, each associated with a specific characteristic of the load. Thus, each component can

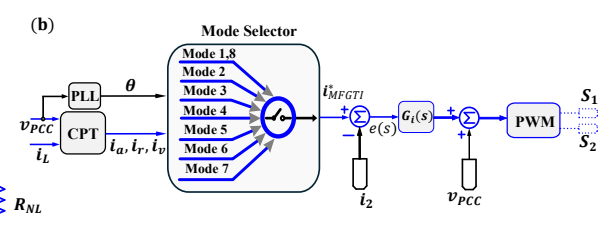


Fig. 1: (a) Overview of MFGTI, (b) block diagram control strategy.

be selected independently (or in combination), enabling selective compensation of current disturbances originating from the load behavior. Furthermore, the MFGTI performs total compensation aiming at mitigating the components that cause current disturbances, using the non-active current as reference, as Table I [2], [3].

TABLE I. CPT MODE SELECTOR CURRENTS.

| Parameter | |
|-----------------------------------|----------------------------------|
| $i_{MFGTI}^{m=1,8} = 0$ | $i_{MFGTI}^{m=2} = i_{GD}$ |
| $i_{MFGTI}^{m=3} = i_L - i_a$ | $i_{MFGTI}^{m=4} = i_r$ |
| $i_{MFGTI}^{m=5} = i_v$ | $i_{MFGTI}^{m=6} = i_{GD} + i_r$ |
| $i_{MFGTI}^{m=7} = -i_{GD} + i_r$ | (180° phase shifted) |

II. SIMULATIONS RESULTS

In order to verify and validate the effectiveness of the proposed control strategy for the single-phase MFGTI, simulations were carried out using the TyphoonSim®. Fig. 2 presents the reference current, i_{ref} , the MFGTI output current, i_{MFGTI} , grid current, i_g , and the scaled PCC voltage, $v_{PCC}/10$, considering all modes of operation. Fig. 2(a) illustrates the reference tracking performed by the MFGTI regardless of the operating mode. In Fig. 2(b), the MFGTI operates in stand-by mode during the first and last scenarios, leading to slightly distorted grid current. In this scenario, the MFGTI exhibits a low λ of 0.66, failing to meet the regulatory requirements, with a total harmonic current distortion rate (THD_{i_2}) of 45.5%. At $t > 0.05$ s, the MFGTI injects only active power without performing compensation, resulting in a grid current that is distorted due to the nonlinear load, consequently leading to a λ lower than 1. In the interval $0.1 < t < 0.15$ s, both reactive power compensation and harmonic mitigation are enabled, yielding a sinusoidal current waveform in phase with the grid voltage. Thus, the MFGTI

operates exclusively as an active filter, resulting in a sinusoidal current from the grid, with a unity λ at the PCC. In the fourth and fifth scenarios, the system performs either reactive compensation or harmonic mitigation, leading to waveform distortion or phase shift between voltage and current, respectively. In the sixth scenario, active current injection is combined with reactive power compensation, resulting in sinusoidal waveform in out-of-phase related to the voltage. It is observed that reactive power compensation increases the THD_{i_2} , as it directly impacts the fundamental component, whereas harmonic mitigation of the load ensures a low THD_{i_2} . On the other hand, the results shows that reactive power compensation ensures a higher λ than current mitigation, as the reactive current component is more significant than the load harmonics. Moreover, during the intervals between the antepenultimate and penultimate ($0.3 < t < 0.35$ s), active power consumption occurs, along with reactive current compensation.

III. CONCLUSIONS

This paper proposed the use of a Type II controller in the inner loop of an MFGTI, enabling active current injection, compensation and mitigation of disturbances caused by a local nonlinear load connected at the PCC. The implemented controller is simple and ensures accurate reference tracking, allowing for selective compensation with the aid of current components derived from CPT. Simulation results demonstrated satisfactory performance across all operating modes, with low tracking errors (below 5%), sinusoidal grid currents, and improved λ . Future work includes comparative analysis of performance with classical control techniques (e.g., hysteresis, PI and Finite State Model Predictive Control) in terms of accuracy, complexity, and robustness and implementation in a laboratory-scale prototype.

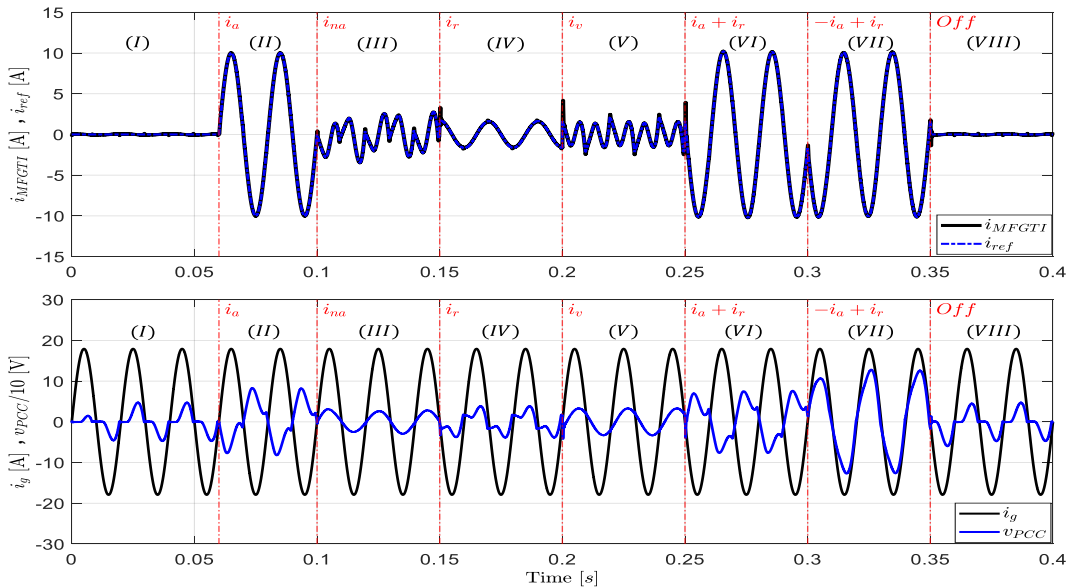


Fig. 2: Current and voltage waveforms. (a) Comparison between the reference current and the current compensated by the MFGTI; (b) Voltage at the PCC and selective current compensation using the CPT.

REFERENCES

- [1] T. D. Curi Busarello, K. Zeb, and M. G. Simões, "Highly Accurate Digital Current Controllers for Single-Phase LCL-Filtered Grid-Connected Inverters," *Electricity*, vol. 1, no. 1, pp. 12–36, Jul. 2020, doi: 10.3390/electricity1010002.

- [2] P. Tenti, H. K. M. Paredes, and P. Mattavelli, "Conservative Power Theory, a Framework to Approach Control and Accountability Issues in Smart Microgrids," *IEEE Trans Power Electron*, vol. 26, no. 3, pp. 664–673, Mar. 2011, doi: 10.1109/TPEL.2010.2093153.
 [3] P. Tenti, A. Costabeber, P. Mattavelli, F. P. Marafao, and H. K. M. Paredes, "Load Characterization and Revenue Metering Under Non-Sinusoidal and Asymmetrical Operation," *IEEE Trans Instrum Meas*, vol. 63, no. 2, pp. 422–431, Feb. 2014, doi: 10.1109/TIM.2013.2280480.